

Non-reciprocal spin-glass transition and aging

Giulia Garcia Lorenzana,^{1,2} Ada Altieri,² Giulio Biroli,¹ Michel Fruchart,³ and Vincenzo Vitelli^{4,5,6}

¹Laboratoire de Physique de l'École normale supérieure, ENS, Université PSL, CNRS, Sorbonne Université, Université de Paris F-75005 Paris, France

²Laboratoire Matière et Systèmes Complexes (MSC), Université Paris Cité, CNRS, 75013 Paris, France

³Gulliver, ESPCI Paris, Université PSL, CNRS, 75005 Paris, France

⁴James Franck Institute, University of Chicago, Chicago, Illinois, 60637, U.S.A.

⁵Department of Physics, University of Chicago, Chicago, Illinois, 60637, U.S.A.

⁶Kadanoff Center for Theoretical Physics, University of Chicago, Chicago, IL 60637, U.S.A.

Disordered systems generically exhibit aging and a glass transition. Previous studies have long suggested that non-reciprocity tends to destroy glassiness. Here, we show that this is not always the case using a bipartite spherical Sherrington-Kirkpatrick model that describes the antagonistic coupling between two identical complex agents modelled as macroscopic spin glasses. Our dynamical mean field theory calculations reveal an exceptional-point mediated transition from a static disorder phase to an oscillating amorphous phase as well as non-reciprocal aging with slow dynamics and oscillations.

Glassy systems do not reach equilibrium even on very long time scales [1–3]. The older the glassy system is, the slower it evolves: the typical relaxation time scale of a sample increases as the time elapsed since its preparation increases [4–6]. This very slow dynamics, known as *aging*, has been observed in physical systems ranging from disordered magnets and spin-glasses to dense liquids and active matter [4–15]. Glass-like dynamics have also been observed in ecological systems [16–23] as well as networks of biological or artificial neurons [24–37]. Notably, these systems can exhibit non-reciprocal interactions between constituents (think of predator-prey relationships in ecology) and therefore need not satisfy micro-reversibility.

Understanding how the dynamics of non-reciprocal systems becomes glassy is a major challenge that goes beyond the body of literature developed in the last decades on glassy systems [38, 39]. Pioneering studies by Crisanti and Sompolinsky (CS) [40] considered a spherical Sherrington-Kirkpatrick (SK) model [41–45] to which they added random *all-to-all* non-reciprocal interactions between spins. They showed that non-reciprocity suppresses the finite temperature spin-glass transition and, hence, also aging dynamics. Instead, chaotic dynamics is observed. These results were extended to more general glassy models in Refs. [46–49] and are believed to originate from the marginal stability of the model (i.e. the presence of flat directions in phase space [50]). The emerging picture is that any amount of non-reciprocal interactions then tends to destroy glassiness.

In this Letter, we demonstrate that the aforementioned conclusions depend on the topology of the network of non-reciprocal interactions, and their distribution. In particular, our analysis accounts for the scenario in which *agents* that are coupled non-reciprocally are themselves macroscopic entities each described by a many-body complex system. Examples include predators and preys, adversarial neural networks or robots, etc. Specifically, we

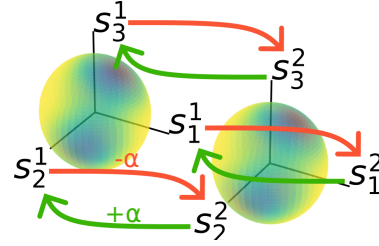


Figure 1: Sketch of the non-reciprocal spin-glass model: two (N -dimensional, in the plot $N = 3$) spherical spin systems, corresponding degrees of freedom are coupled non-reciprocally. The sphere's colors sketch the identical random potential in both systems.

consider a bipartite many-body spin-glass system representing two (type of) agents with non-reciprocal interactions. We find evidence of (i) a finite temperature non-reciprocal spin-glass phase transition between a static disordered phase and a time-dependent amorphous phase and (ii) non reciprocal aging characterized by both slow dynamics and oscillations. The mechanism underpinning the destabilization of the usual spin glass in favour of the non-reciprocal one is a spectral singularity called exceptional point.

Non-reciprocal interactions considered here have been studied in a variety of contexts where they generate a rich phenomenology ranging from oscillatory states and travelling waves [51–59] to chaotic states [27, 29, 40, 60, 61] and nonequilibrium phase transitions [51, 56, 62? ? – 67]. In the context of spin glasses, it has been shown in Ref. [68] that the oscillatory dynamics often encountered in this class of systems persists in mean-field Mattis-like models in which disorder can be gauged away by a change of variables [69, 70]. However, these systems are not marginal, leaving open the question of how non-reciprocity affects marginally stable glassy systems.

Model.— To construct a minimal model exhibiting marginal glassy dynamics in the absence of non-reciprocity, we follow the route of Crisanti and Sompolinsky but with a crucial difference. We consider *two* spherical (SK) spin-glass systems each composed of N spins representing two distinct species denoted by 1 and 2 with random all-to-one symmetric interactions within the same species plus a non-reciprocal (i.e. asymmetric) deterministic coupling between the two species. This setup is described by the Langevin dynamics:

$$\begin{cases} \dot{s}_i^1 = \sum_j J_{ij} s_j^1 - \ell_1 s_i^1 + \alpha s_i^2 + \eta_i^1 \\ \dot{s}_i^2 = \sum_j J_{ij} s_j^2 - \ell_2 s_i^2 - \alpha s_i^1 + \eta_i^2 \end{cases} \quad (1)$$

in which s_i^a is the state of the spin $i = 1, \dots, N$ in the system $a = 1, 2$. The quenched interaction matrix J_{ij} is symmetrical and initially assumed to be the same in both systems (see model extensions). The elements of J_{ij} are drawn from a Gaussian distribution with zero mean and variance σ^2/N ($\sigma = 1$ in the following). The spins s_i^1 and s_i^2 in each system are coupled anti-symmetrically, with a coupling strength α : system 1 wants to align with system 2, whereas system 2 wants to anti-align with system 1. These non-reciprocal interactions correspond to attraction and repulsion between 1 and 2. See Figure 1 for a graphical sketch. Each spin is also subject to a thermal Gaussian white noise η_i^a with covariance $\langle \eta_i^a(t) \eta_j^b(t') \rangle = 2T \delta_{ij} \delta_{ab} \delta(t-t')$, where T denotes the temperature. Finally, ℓ_1 and ℓ_2 are Lagrange multipliers used to enforce the spherical constraints $\frac{1}{N} \sum_{i=1}^N (s_i^a)^2 = 1$. This model can be interpreted as describing the dynamics of two identical agents that are antagonistically coupled and whose internal complexity is modelled by spin-glass dynamics.

Non-reciprocal spin-glass transition — Without non-reciprocity, the spherical spin-glass model displays a finite temperature phase transition between a high-temperature disordered phase and a low-temperature ordered phase. The latter is characterized by two ground states related by spin-inversion symmetry (in replica language, it reflects a simple replica symmetric spin-glass phase) [43, 45]. The transition can also be detected dynamically: starting from random initial conditions, the system converges to a steady state, whose relaxation time diverges when approaching T_c . In the following, we analyze the effect of non-reciprocity on the steady-state dynamics by progressively decreasing the temperature.

In the thermodynamic limit $N \rightarrow \infty$, the dynamics of the system can be analyzed by Dynamical Mean-Field Theory (DMFT) [40, 71–73]. By applying DMFT (SM), we find two coupled self-consistent equations for a given couple s_i^1, s_i^2 . Since the resulting equation does not depend on i , we drop the index i in the following and rewrite the equation in vectorial form as:

$$\dot{\mathbf{s}} = -\Lambda \mathbf{s} + \alpha \epsilon \mathbf{s} + \xi + \int_0^t dt' R(t, t') \mathbf{s}(t'), \quad (2)$$

where $\mathbf{s} = [s^1, s^2]^T$ is a two-dimensional vector that contains the two spins, $\Lambda = \text{diag}(\ell_1, \ell_2)$ is the diagonal matrix of the Lagrange multipliers, ϵ is the fully antisymmetric Levi-Civita symbol. The noise vector ξ is Gaussian with zero mean and variance $\langle \xi_a(t) \xi_b(t') \rangle = 2T \delta_{ab} \delta(t-t') + C_{ab}(t, t')$. Finally,

$$C_{ab}(t, t') = \langle s_a(t) s_b(t') \rangle, \quad R_{ab}(t, t') = \frac{\partial \langle s_a(t) \rangle}{\partial h_b(t')}. \quad (3)$$

are the average correlation and response matrices, which have to be determined self-consistently. At high temperature, the system reaches a time-translation invariant (TTI) state (see SM). We can then compactly write the self-consistent equations for the correlation C and the response R in Fourier space:

$$R^{-1}(\omega) = (-i\omega + \ell) \mathbb{1} - R(\omega) - \alpha \epsilon \quad (4)$$

$$C(\omega) = 2T((R(\omega)^\dagger R(\omega))^{-1} - \mathbb{1})^{-1}, \quad (5)$$

where ℓ is the value of the two Lagrange multipliers, which are constant and equal in the TTI regime. Note that because the system is symmetric under the transformation $s_1 \rightarrow -s_2, s_2 \rightarrow s_1$, both R and C have only two independent elements: the diagonal elements are equal, whereas the off-diagonal ones are equal and opposite. Also, because of the spherical constraint, the autocorrelation function must equal 1 for $t = 0$.

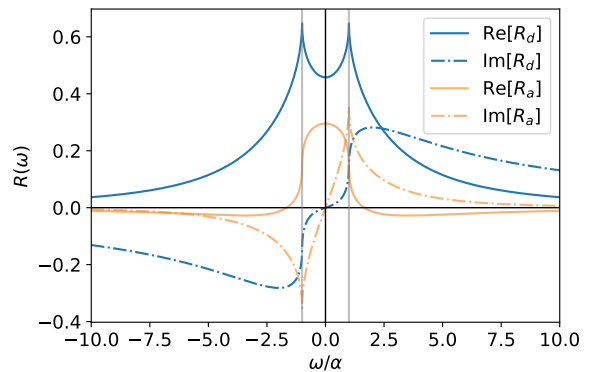


Figure 2: Real and imaginary part of the diagonal (R_d) and antisymmetric (R_a) components of the response function R at the critical point. In grey we highlight $\omega/\alpha = \pm 1$. $\alpha = 0.7, T = T_c = 1$.

By solving these equations (SM) we find that both response and correlation functions are peaked around $\omega = \pm\alpha$ (see Fig. 2 for $R(\omega)$ and SM for $C(\omega)$). This is the frequency at which the system would exhibit regular oscillations in the absence of disordered interactions. Strikingly, in their presence, the disordered system does not exhibit macroscopic oscillations but responds more strongly if excited at this frequency. These peaks lead to bona-fide singularities when $T \rightarrow T_c = 1$: the one

of $R(\omega)$ approaches a finite limit with a square root behaviour (Figure 2), whereas the one of $C(\omega)$ diverges as $(\omega \mp \alpha)^{-1/2}$. In the time domain, one finds a relaxation time to the non-equilibrium steady state that diverges as $1/\sqrt{T - T_c}$ and critical relaxation at T_c , corresponding to a behavior $C(t) \sim \cos(\alpha t)/t^{1/2}$.

This transition shares crucial similarities to the transition to an ordinary spin glass phase that is found in the reciprocal (uncoupled) case except for the superposition of oscillations that shift the singularity of correlation and response functions from $\omega = 0$ to $\omega = \pm\alpha$. The self-consistency equations in terms of the eigenvalues of R and C can be shown (SM) to reduce exactly to the ones obtained in the uncoupled case, except for a shift of $+\alpha$ or $-\alpha$ in the ω dependence of the two eigenvalues. This mapping explains why the critical behaviour and even the critical point $T_c = 1$ are the same as in the uncoupled case. The analysis of the steady state dynamics therefore reveals a first important result: adding non-reciprocal interactions to the spherical spin-glass model does lead to a dynamical phase transition, which generalizes the spin-glass transition found in the symmetric case. This is in contrast with what is found for all-to-all non-reciprocal interactions à la CS, which instead wipe out the finite temperature transition [40]. We will now show that the different form of non-reciprocity also leads to a very different physical behavior for the non-equilibrium dynamics.

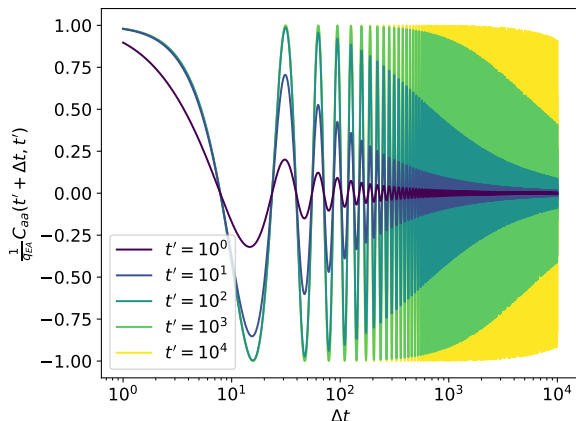


Figure 3: Diagonal component of the correlation function, normalized by the Edward-Anderson order parameter, for different values of the waiting time.

Non-reciprocal aging — Since the relaxation time diverges at T_c , the dynamics after quenches below T_c are not expected to relax to a steady state. As we show below, indeed they do not — instead aging ensues (on timescales that do not diverge with N). To study the aging regime we follow Ref. [43] and analyze the dynamics in the basis that diagonalizes the interaction matrix J .

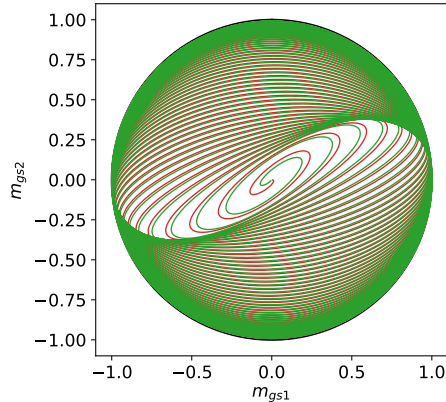


Figure 4: Projection on the two leading eigenvectors of the interaction matrix J of the trajectories (green and red) of the two systems. Random initial conditions (center) at zero temperature; $N = 20000$, $t_{max} = 2000$.

This leads to

$$\dot{\mathbf{s}}_\mu = (\mu\mathbb{1} - \Lambda + \alpha\epsilon)\mathbf{s}_\mu + \xi_\mu \quad (6)$$

in which the eigenvalues μ of J are used to label the two-dimensional vectors \mathbf{s}^μ composed of the projections of s^1 and s^2 on the corresponding eigenvector. The different modes are now coupled only through the Lagrange multipliers. At $t = 0$ each mode is initialized as a Gaussian random variable with mean zero and variance one, corresponding to a sudden quench from infinite temperature to the temperature T . Using a procedure similar to Ref. [43] we find that after the quench \mathbf{s}_μ rotates at constant angular velocity α , while its radius undergoes a slow aging evolution akin to the one found in the absence of non-reciprocity (SM). The self-correlation functions, C_{11} and C_{22} , plotted in Figure 3 for different values of the initial time t' , read in the asymptotic regime $t, t' \gg 1$, $\Delta t = t - t' \gg 1$:

$$C_{aa}(t, t') = q_{EA} \left(\frac{2\sqrt{1 + \Delta t/t'}}{2 + \Delta t/t'} \right)^{3/2} \cos(\alpha\Delta t) \quad (7)$$

where $q_{EA} = 1 - \frac{T}{T_c}$ is the non-reciprocal counterpart of the Edwards-Anderson order parameter or self-overlap [43, 45, 74, 75] (see SM for the expression for $C_{ab}(t, t')$). This form is in very good agreement with the simulation results (SM). In summary, in the non-reciprocal case, the correlation function after a quench displays both an oscillating behavior due to non-reciprocal interactions and a slow aging evolution – with a dependence on $\Delta t/t'$, which remarkably turns out to be the same as in the reciprocal case [43, 45].

Asymptotic behaviour — Let us now consider the asymptotic behavior, i.e. the regime $t \rightarrow \infty$ at fixed but

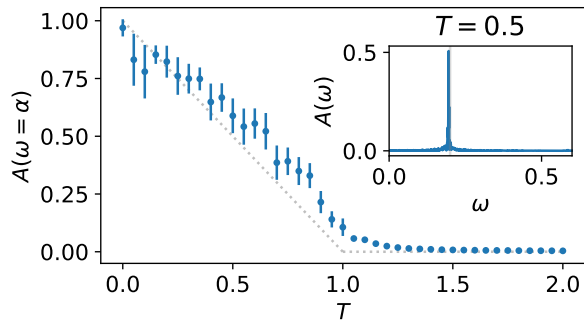


Figure 5: Numerical results for the amplitude of the Fourier component at $\omega = \alpha$ of the projection of one of the two clones on the leading eigenvector, as a function of temperature. The amplitude goes to zero continuously for $T \rightarrow T_c = 1$; in grey we show $q_{EA} = 1 - \frac{T}{T_c}$. In the inset, the amplitude of the Fourier transform as a function of ω for $T = 0.5$.

large N . In the $\alpha = 0$ case, the system equilibrates to one of the two pure states associated with spin configurations oriented in the direction of the leading eigenvector of J , denoted as v_{μ_0} , and then on time-scales exponentially large in $N^{1/3}$ [76, 77] the system switches from one state to the other by activated barrier hopping. By numerically integrating the equations of motion (1), we find that the situation changes drastically once α is switched on. Activated barrier hopping is wiped out by the non-reciprocity and each of the systems oscillates on timescales of order one between the two states. More precisely, at zero temperature each system performs a periodic orbit in the circle spanned by the two lowest eigenvalues of J (Figure 4) with angular frequency α and relative phase $\pi/2$. At finite temperature, the Fourier transform of the projection of the spin configuration of any of the two systems on the leading eigenvector has a delta peak in $\omega = \alpha$, whose amplitude $A(\omega = \alpha)$ goes to zero continuously at the transition (Figure 5). This oscillating phase, which we call non-reciprocal spin-glass, is the counterpart of the low-temperature static phase found at equilibrium. The observable $A(\omega = \alpha)$ is related to the non-reciprocal Edwards-Anderson parameter q_{EA} . Its numerical dependence on temperature indicates a phase transition at T_c [78].

Exceptional-point mediated transition — To investigate analytically the existence of the oscillating phase described above, we now analyze the stability of the equilibrium points at zero temperature. In the presence of non-reciprocal forces, $\pm\sqrt{N}v_{\mu_0}$ are still equilibrium points for both systems. We study their stability by linearizing the dynamics (6) around them (we stick to the case $s^1 = s^2 = \sqrt{N}v_{\mu_0}$ for simplicity). The stability matrix is block diagonal in the basis that diagonalizes J . For each μ the corresponding block in the stability matrix reads

$$(SM) \quad M_\mu = \begin{pmatrix} \mu - \mu_0 - \alpha & \alpha \\ -\alpha & \mu - \mu_0 + \alpha \end{pmatrix} \quad (8)$$

The matrix M_μ is not diagonalizable, because it has only one eigenvector $(1, 1)^\top$ (instead of two). This situation is known as an exceptional point. The corresponding eigenvalue $\lambda = \mu - \mu_0$ is always positive because μ_0 is the lowest eigenvalue of J . Nevertheless, for non-normal matrices (such as those close to or at an exceptional point), looking at the eigenvalues of the stability matrix is not sufficient to determine the behavior of the system around the equilibrium point [79]. We find by solving the linearized dynamics (SM) that a perturbation on the mode μ is initially amplified as long as $\mu - \mu_0 < \alpha$, although M_μ has only non-negative eigenvalues. In the thermodynamic limit, the gap between the first and subsequent eigenvalues vanishes, therefore for any finite value of α there will be an extensive number of unstable modes destabilizing the condensed phase. This mechanism changes the nature of the low-temperature regime compared to the equilibrium case, and it leads to the rotating non-reciprocal spin-glass phase studied here. This exceptional-point mediated transition is reminiscent of the non-reciprocal phase transitions studied in Ref. [56]. Our results provide an extension of that mechanism to simple disordered systems.

Because of the non-reciprocity-related instability, each system rotates in the very long time limit. In the equilibrium case, there is a symmetry breaking corresponding to the choice of one of the two pure states. In the non-reciprocal case, there is spontaneous chiral symmetry breaking: the direction of rotation is randomly selected, and with a rotation plane that is disorder-dependent. As a result, similarly to what was found in references [68, 80] for a related model, the oscillations are not visible in the magnetization of the system, that is zero in this phase, or other disorder-independent one-time observables. Instead, they are visible in the auto-correlation function [81].

Model extensions — We emphasize that our non-reciprocal coupling α introduces a unique timescale for oscillations, in contrast with the random non-reciprocity in CS model, which leads to a continuous timescale distribution. Indeed, for continuous distributions of random anti-symmetrical coupling α_i (see SM), we find that the transition is suppressed at any finite temperature destroying the aging behaviour and leading to chaotic dynamics as in the CS model. For a continuous but sharp distribution, a sharp crossover is expected, that would be indistinguishable from a phase transition except in extremely large systems at extremely long times. In this case the system would display interrupted aging, i.e. aging only up to extremely large time-scales [4]. We have also considered anti-symmetric couplings which can only assume two different values with different probabil-

ities. In this case, a genuine transition still exists. This raises the intriguing possibility of two different scenarios for non-reciprocal interactions: (i) one characteristic of continuous distributions first evidenced by Crisanti and Sompolinsky, (ii) one characteristic of discrete distributions, whose simplest incarnation is the system analyzed in this paper. Physically, continuous vs discrete distributions indeed correspond to quite different situations. The latter can be seen as macroscopic sub-systems coupled with different non-reciprocal interactions.

As a further extension, we considered the case when the two species have different interaction matrices J_{ij}^{α} with a degree of correlation ρ (SM). The response and correlation functions exhibit damped oscillating behavior but only for α above some (ρ -dependent) finite threshold. The finite temperature transition is suppressed but for high values of α the low temperature behavior resembles the one of the non-reciprocal spin glass phase up to moderately large time-scales (SM). We also studied the case in which the two systems are non-reciprocally coupled through their respective magnetizations: system 1 wants to align with the magnetization of system 2, whereas system 2 does the opposite. For strong ferromagnetic interactions, the model displays two distinct oscillating phases and non-reciprocal aging (SM).

Finally, we performed preliminary numerical simulations of two non-reciprocally coupled spherical spin-glass systems with 3-body random interactions [82, 83], which capture some features of the glass transition in supercooled liquids. Aging persists on the accessible timescales, which are larger than $1/\alpha$ (SM). In this case, we expect no regular oscillations to occur [84] and the critical temperature (or the sharp cross-over towards interrupted aging) to decrease with α .

To sum up, by studying minimal spin-glass models, we have shown that non-reciprocal interactions between two distinct species can lead to an exceptional-point mediated spin-glass phase and a novel mechanism of non-reciprocal aging with potential implications for many-body systems in which complex agents with antagonistic goals are themselves modelled as macroscopic disordered systems.

We thank Y. Fyodorov for interesting discussions. This work was supported by the Simons Foundation Grant No. 454935 (G.B.). A.A. acknowledges the support received from the Agence Nationale de la Recherche (ANR) of the French government, under the grant ANR-23-CE30-0012-01 (SIDECAR project). M.F. acknowledges partial support from the National Science Foundation under grant DMR-2118415, a Kadanoff–Rice fellowship funded by the National Science Foundation under award no. DMR-2011854 and the Simons Foundation. V.V. acknowledges partial support from the Army Research Office under grant W911NF-22-2-0109 and W911NF-23-1-0212 and the Chan Zuckerberg Initiative. M.F. and V.V. acknowledge partial support from the France Chicago cen-

ter through a FACCTS grant. This research was partly supported from the National Science Foundation through the Center for Living Systems (grant no. 2317138) and the National Institute for Theory and Mathematics in Biology (NITMB).

-
- [1] *Slow Relaxations and nonequilibrium dynamics in condensed matter: Les Houches Session LXXVII, 1-26 July, 2002* (Springer Berlin Heidelberg, 2003).
 - [2] N. C. Keim, J. D. Paulsen, Z. Zeravcic, S. Sastry, and S. R. Nagel, Memory formation in matter, *Reviews of Modern Physics* **91**, 035002 (2019).
 - [3] F. Arceri, F. P. Landes, L. Berthier, and G. Biroli, A statistical mechanics perspective on glasses and aging, in *Encyclopedia of Complexity and Systems Science* (Springer Berlin Heidelberg, 2021) p. 1–68.
 - [4] J.-P. Bouchaud, L. F. Cugliandolo, J. Kurchan, and M. Mézard, Out of equilibrium dynamics in spin-glasses and other glassy systems, in *Spin Glasses and Random Fields*, Series on Directions in Condensed Matter Physics, Vol. Volume 12 (WORLD SCIENTIFIC, 1997) pp. 161–223.
 - [5] G. Biroli, A crash course on ageing, *Journal of Statistical Mechanics: Theory and Experiment* **2005**, P05014 (2005).
 - [6] L. F. Cugliandolo, Course 7: Dynamics of Glassy Systems, in *Slow Relaxations and Nonequilibrium Dynamics in Condensed Matter*, edited by J.-L. Barrat, M. Feigelman, J. Kurchan, and J. Dalibard (Springer, Berlin, Heidelberg, 2003) pp. 367–521.
 - [7] L. Berthier and G. Biroli, Theoretical perspective on the glass transition and amorphous materials, *Reviews of modern physics* **83**, 587 (2011).
 - [8] L. Berthier and J. Kurchan, Non-equilibrium glass transitions in driven and active matter, *Nature Physics* **9**, 310 (2013).
 - [9] Y.-E. Keta, R. L. Jack, and L. Berthier, Disordered collective motion in dense assemblies of persistent particles, *Physical Review Letters* **129**, 048002 (2022).
 - [10] L. M. C. Janssen, Active glasses, *Journal of Physics: Condensed Matter* **31**, 503002 (2019), publisher: IOP Publishing.
 - [11] L. Berthier, E. Flenner, and G. Szamel, Glassy dynamics in dense systems of active particles, *The Journal of Chemical Physics* **150**, 200901 (2019).
 - [12] F. Ghimenti, L. Berthier, G. Szamel, and F. van Wijland, Transverse forces and glassy liquids in infinite dimensions, *Physical Review E* **109**, 064133 (2024).
 - [13] F. Ghimenti, L. Berthier, and F. van Wijland, Irreversible monte carlo algorithms for hard disk glasses: From event-chain to collective swaps, *Physical Review Letters* **133**, 028202 (2024).
 - [14] F. Ghimenti, L. Berthier, G. Szamel, and F. van Wijland, Sampling efficiency of transverse forces in dense liquids, *Physical Review Letters* **131**, 257101 (2023).
 - [15] R. Mandal and P. Sollich, Multiple types of aging in active glasses, *Physical Review Letters* **125**, 218001 (2020).
 - [16] A. Altieri, F. Roy, C. Cammarota, and G. Biroli, Properties of Equilibria and Glassy Phases of the Random Lotka-Volterra Model with Demographic Noise, *Physical*

- Review Letters **126**, 258301 (2021).
- [17] A. Altieri and G. Biroli, Effects of intraspecific cooperative interactions in large ecosystems, *SciPost Physics* **12**, 013 (2022).
- [18] A. Altieri, Glassy features and complex dynamics in ecological systems (2022), arXiv:2208.14956.
- [19] M. Loreau and C. de Mazancourt, Biodiversity and ecosystem stability: A synthesis of underlying mechanisms, *Ecology Letters* **16**, 106 (2013).
- [20] S. Allesina and S. Tang, Stability criteria for complex ecosystems, *Nature* **483**, 205 (2012).
- [21] T. Galla, Random replicators with asymmetric couplings, *Journal of Physics A: Mathematical and General* **39**, 3853 (2006).
- [22] V. Ros, F. Roy, G. Biroli, G. Bunin, and A. M. Turner, Generalized Lotka-Volterra Equations with Random, Nonreciprocal Interactions: The Typical Number of Equilibria, *Physical Review Letters* **130**, 257401 (2023).
- [23] T. Arnoux de Pirey and G. Bunin, Many-species ecological fluctuations as a jump process from the brink of extinction, *Physical Review X* **14**, 011037 (2024).
- [24] J. J. Hopfield, Neural networks and physical systems with emergent collective computational abilities., *Proceedings of the National Academy of Sciences* **79**, 2554–2558 (1982).
- [25] J. A. Hertz, G. Grinstein, and S. A. Solla, Memory networks with asymmetric bonds, in *AIP Conference Proceedings* (AIP, 1986).
- [26] P. Dayan and L. F. Abbott, *Theoretical Neuroscience: Computational and Mathematical Modeling of Neural Systems*, Computational Neuroscience (Massachusetts Institute of Technology Press, Cambridge, Mass, 2001).
- [27] H. Sompolinsky, A. Crisanti, and H. J. Sommers, Chaos in Random Neural Networks, *Physical Review Letters* **61**, 259 (1988).
- [28] G. Parisi, Asymmetric neural networks and the process of learning, *Journal of Physics A: Mathematical and General* **19**, L675 (1986).
- [29] C. Martorell, R. Calvo, A. Annibale, and M. A. Muñoz, Dynamically selected steady states and criticality in non-reciprocal networks (2023), arXiv:2312.12039 [cond-mat].
- [30] B. Derrida, E. Gardner, and A. Zippelius, An Exactly Solvable Asymmetric Neural Network Model, *Europhysics Letters (EPL)* **4**, 167 (1987).
- [31] F. Aguirre-López, M. Pastore, and S. Franz, Satisfiability transition in asymmetric neural networks, *Journal of Physics A: Mathematical and Theoretical* **55**, 305001 (2022).
- [32] D. G. Clark and L. F. Abbott, Theory of coupled neuronal-synaptic dynamics, *Physical Review X* **14**, 021001 (2024).
- [33] D. Martí, N. Brunel, and S. Ostojic, Correlations between synapses in pairs of neurons slow down dynamics in randomly connected neural networks, *Physical Review E* **97**, 062314 (2018).
- [34] D. Dahmen, S. Grün, M. Diesmann, and M. Helias, Second type of criticality in the brain uncovers rich multiple-neuron dynamics, *Proceedings of the National Academy of Sciences* **116**, 13051–13060 (2019).
- [35] G. Biroli and M. Mézard, Generative diffusion in very large dimensions, *Journal of Statistical Mechanics: Theory and Experiment* **2023**, 093402 (2023).
- [36] G. Biroli, T. Bonnaire, V. de Bortoli, and M. Mézard, Dynamical regimes of diffusion models (2024), arXiv:2402.18491.
- [37] M. Baity-Jesi, L. Sagun, M. Geiger, S. Spigler, G. B. Arous, C. Cammarota, Y. LeCun, M. Wyart, and G. Biroli, Comparing dynamics: Deep neural networks versus glassy systems, in *Proceedings of the 35th International Conference on Machine Learning*, Proceedings of Machine Learning Research, Vol. 80, edited by J. Dy and A. Krause (PMLR, 2018) pp. 314–323.
- [38] M. Mezard, G. Parisi, and M. Virasoro, *Spin Glass Theory and Beyond: An Introduction to the Replica Method and Its Applications*, World Scientific Lecture Notes in Physics, Vol. 9 (WORLD SCIENTIFIC, 1986).
- [39] P. Charbonneau, E. Marinari, G. Parisi, F. Ricci-Tersenghi, G. Sicuro, F. Zamponi, and M. Mezard, *Spin Glass Theory And Far Beyond: Replica Symmetry Breaking After 40 Years* (World Scientific Publishing Company, 2023).
- [40] A. Crisanti and H. Sompolinsky, Dynamics of spin systems with randomly asymmetric bonds: Langevin dynamics and a spherical model, *Physical Review A* **36**, 4922 (1987).
- [41] D. Sherrington and S. Kirkpatrick, Solvable model of a spin-glass, *Physical Review Letters* **35**, 1792–1796 (1975).
- [42] G. Parisi, Infinite number of order parameters for spin-glasses, *Physical Review Letters* **43**, 1754–1756 (1979).
- [43] L. F. Cugliandolo and D. S. Dean, Full dynamical solution for a spherical spin-glass model, *Journal of Physics A: Mathematical and General* **28**, 4213 (1995).
- [44] J. M. Kosterlitz, D. J. Thouless, and R. C. Jones, Spherical Model of a Spin-Glass, *Physical Review Letters* **36**, 1217 (1976).
- [45] C. De Dominicis and I. Giardinà, *Random Fields and Spin Glasses* (Cambridge University Press, Cambridge, 2006).
- [46] L. F. Cugliandolo, J. Kurchan, P. Le Doussal, and L. Peliti, Glassy behaviour in disordered systems with nonrelaxational dynamics, *Physical review letters* **78**, 350 (1997).
- [47] L. Berthier, J.-L. Barrat, and J. Kurchan, A two-time-scale, two-temperature scenario for nonlinear rheology, *Physical Review E* **61**, 5464 (2000).
- [48] H. Horner, Drift, creep and pinning of a particle in a correlated random potential, *Zeitschrift für Physik B Condensed Matter* **100**, 243 (1996).
- [49] Y. V. Fyodorov, E. Gudowska-Nowak, M. A. Nowak, and W. Tarnowski, Non-orthogonal eigenvectors, fluctuation-dissipation relations and entropy production, arXiv e-prints, arXiv (2023).
- [50] M. Müller and M. Wyart, Marginal stability in structural, spin, and electron glasses, *Annu. Rev. Condens. Matter Phys.* **6**, 177 (2015).
- [51] Y. Avni, M. Fruchart, D. Martin, D. Seara, and V. Vitelli, The non-reciprocal Ising model (2023), arXiv:2311.05471 [cond-mat, physics:nlm].
- [52] L. Guislain and E. Bertin, Collective oscillations in a three-dimensional spin model with non-reciprocal interactions (2024), arXiv:2405.13925 [cond-mat].
- [53] L. Guislain and E. Bertin, Discontinuous phase transition from ferromagnetic to oscillating states in a nonequilibrium mean-field spin model (2023), arXiv:2310.13488 [cond-mat].
- [54] L. Guislain and E. Bertin, Nonequilibrium Phase Transition to Temporal Oscillations in Mean-Field Spin Models,

- Physical Review Letters **130**, 207102 (2023).
- [55] D. Martin, D. Seara, Y. Avni, M. Fruchart, and V. Vitelli, An exact model for the transition to collective motion in nonreciprocal active matter (2023), arXiv:2307.08251 [cond-mat].
- [56] M. Fruchart, R. Hanai, P. B. Littlewood, and V. Vitelli, Non-reciprocal phase transitions, *Nature* **592**, 363 (2021).
- [57] S. Saha, J. Agudo-Canalejo, and R. Golestanian, Scalar Active Mixtures: The Nonreciprocal Cahn-Hilliard Model, *Physical Review X* **10**, 041009 (2020).
- [58] Z. You, A. Baskaran, and M. C. Marchetti, Nonreciprocity as a generic route to traveling states, *Proceedings of the National Academy of Sciences* **117**, 19767 (2020).
- [59] S. A. M. Loos, S. H. L. Klapp, and T. Martynec, Long-range order and directional defect propagation in the nonreciprocal xy model with vision cone interactions, *Physical Review Letters* **130**, 198301 (2023).
- [60] A. Dinelli, J. O’Byrne, A. Curatolo, Y. Zhao, P. Sollich, and J. Tailleur, Non-reciprocity across scales in active mixtures, *Nature Communications* **14**, 7035 (2023).
- [61] R. Zakine, J. Garnier-Brun, A.-C. Becharat, and M. Benzaquen, Socioeconomic agents as active matter in nonequilibrium Sakoda-Schelling models, *Physical Review E* **109**, 044310 (2024).
- [62] R. Hanai, Nonreciprocal frustration: Time crystalline order-by-disorder phenomenon and a spin-glass-like state, *Physical Review X* **14**, 011029 (2024).
- [63] R. Daviet, C. P. Zelle, A. Rosch, and S. Diehl, Nonequilibrium Criticality at the Onset of Time-Crystalline Order, *Physical Review Letters* **132**, 167102 (2024), arXiv:2312.13372 [cond-mat].
- [64] C. P. Zelle, R. Daviet, A. Rosch, and S. Diehl, Universal phenomenology at critical exceptional points of nonequilibrium o(n) models, *Physical Review X* **14**, 021052 (2024).
- [65] B. Ottino-Löffler and S. H. Strogatz, Volcano Transition in a Solvable Model of Frustrated Oscillators, *Physical Review Letters* **120**, 264102 (2018).
- [66] A. Prüser, S. Rosmej, and A. Engel, Nature of the Volcano Transition in the Fully Disordered Kuramoto Model, *Physical Review Letters* **132**, 187201 (2024), arXiv:2310.09079 [cond-mat, physics:nlin].
- [67] A. Prüser and A. Engel, Role of Coupling Asymmetry in the Fully Disordered Kuramoto Model (2024), arXiv:2408.12988 [cond-mat, physics:nlin].
- [68] L. Guislain and E. Bertin, Hidden collective oscillations in a disordered mean-field spin model with non-reciprocal interactions (2024), arXiv:2406.03874 [cond-mat].
- [69] D. Mattis, Solvable spin systems with random interactions, *Physics Letters A* **56**, 421–422 (1976).
- [70] G. Toulouse *et al.*, Theory of the frustration effect in spin glasses: I, *Spin Glass Theory and Beyond: An Introduction to the Replica Method and Its Applications* **9**, 99 (1987).
- [71] H. Sompolinsky and A. Zippelius, Relaxational dynamics of the Edwards-Anderson model and the mean-field theory of spin-glasses, *Physical Review B* **25**, 6860 (1982).
- [72] A. Altieri, G. Biroli, and C. Cammarota, Dynamical mean-field theory and aging dynamics, *Journal of Physics A: Mathematical and Theoretical* **53**, 375006 (2020).
- [73] L. F. Cugliandolo, Recent Applications of Dynamical Mean-Field Methods (2023), arXiv:2305.01229 [cond-mat].
- [74] S. F. Edwards and P. W. Anderson, Theory of spin glasses, *Journal of Physics F: Metal Physics* **5**, 965 (1975).
- [75] G. Parisi, THE OVERLAP IN GLASSY SYSTEMS, in *Stealing the Gold: A Celebration of the Pioneering Physics of Sam Edwards*, edited by D. Sherrington, P. Goldbart, and N. Goldenfeld (Oxford University Press, 2004) p. 192–211.
- [76] G. J. Rodgers and M. A. Moore, Distribution of barrier heights in infinite-range spin glass models, *Journal of Physics A: Mathematical and General* **22**, 1085 (1989).
- [77] D. Barbier, P. H. De Freitas Pimenta, L. F. Cugliandolo, and D. A. Stariolo, Finite size effects and loss of self-averageness in the relaxational dynamics of the spherical Sherrington-Kirkpatrick model, *Journal of Statistical Mechanics: Theory and Experiment* **2021**, 073301 (2021).
- [78] The way the non-reciprocal spin-glass phase disappears at T_c ($A(\omega = \alpha) \rightarrow 0$) is quantitatively similar to the way the condensed (on v_{μ_0}) phase disappears ($q_{EA} \rightarrow 0$) in the reciprocal (uncoupled) case.
- [79] L. N. Trefethen and M. Embree, *Spectra and Pseudospectra: The Behavior of Nonnormal Matrices and Operators* (Princeton University Press, Princeton, N.J, 2005).
- [80] L. Guislain and E. Bertin, Far-from-equilibrium complex landscapes (2024), arXiv:2405.08452 [cond-mat].
- [81] In practice, to determine the plane of rotation one can perform a principal component analysis (PCA) of the trajectory of the system.
- [82] A. Crisanti and H. J. Sommers, The spherical spin interaction spin glass model: The statics, *Zeitschrift für Physik B Condensed Matter* **87**, 341 (1992).
- [83] L. F. Cugliandolo and J. Kurchan, Analytical solution of the off-equilibrium dynamics of a long-range spin-glass model, *Physical Review Letters* **71**, 173 (1993).
- [84] In this case, saddles with few unstable directions are not related by inversion symmetry, with simple zero modes connecting them.
- [85] M. Potters and J.-P. Bouchaud, *A First Course in Random Matrix Theory: For Physicists, Engineers and Data Scientists* (Cambridge University Press, Cambridge, 2020).

Dynamical Mean Field Theory

The effective dynamical equations for a single representative spin for each clone can be derived through Dynamical Mean Field Theory. The derivation is standard, but we sketch it here for the convenience of the reader.

The starting point are the equations defining the dynamics of our system:

$$\dot{s}_i^a = \sum_{j=1}^N J_{ij} s_j^a - \ell_a s_i^a + \sum_b \alpha \epsilon_{ab} s_i^b + \eta_i^a + h_i^a \quad (9)$$

where we have also included a field on each spin that will be taken to be zero at the end of the computation. Given noise realization $\eta_i^a(t)$, these equations define the trajectories $s_i^a(t)$.

We can now add a new spin, with index 0, to each of the clones, and draw their initial conditions and interactions independently from the rest of the system. Since the interactions with each of the other components are of order $1/\sqrt{N}$, its introduction can be considered a small perturbation, and we can compute the linear response of the system to it, $\delta s_i^a(t)$:

$$\delta s_i^a(t) = \sum_{b,j} \int_0^t dt' \frac{\delta s_i^a(t)}{\delta h_j^b(t')} J_{j0} s_0^b(t') = \sum_{b,j} \int_0^t dt' R_{ij}^{ab}(t, t') J_{j0} s_0^b(t') \quad (10)$$

The dynamics of spins 0 will depend on the new trajectories of all the others:

$$\dot{s}_0^a = \sum_{j=0}^N J_{0j} (s_j^a + \delta s_j^a) - \ell_a s_0^a + \sum_b \alpha \epsilon_{ab} s_0^b + \eta_0^a + h_0^a \quad (11)$$

We now want to describe the statistic of the interaction term in the limit $N \rightarrow \infty$. The unperturbed trajectories are by definition uncorrelated from the interactions with 0, they contribute a colored noise $\sum_j J_{0j} s_j^a \sim \xi_a$ with statistics:

$$\langle \xi_a(t) \rangle = 0 \quad \langle \xi_a(t) \xi_b(t') \rangle = \mathbb{E} [s_i^a(t) s_i^b(t')] = C_{ab}(t, t') \quad (12)$$

The perturbation of the trajectories is instead correlated to the interactions with 0:

$$\sum_i J_{0i} \delta s_i^a = \sum_i J_{0i} \sum_{j,b} J_{j0} \int_0^t dt' R_{ij}^{ab}(t, t') s_0^b(t') \sim \sum_b \int_0^t dt' \overline{R_{jj}^{ab}(t, t')} s_0^b(t') = \sum_b \int_0^t dt' R_{ab}(t, t') s_0^b(t') \quad (13)$$

Substituting in the dynamics for s_0^a :

$$\dot{s}_0^a = -\ell_a s_0^a + \sum_b \alpha \epsilon_{ab} s_0^b + \eta_0^a + h_0^a + \xi_a + \sum_b \int_0^t dt' R_{ab}(t, t') s_0^b(t') \quad (14)$$

Since spins 0 are equivalent to all others, we can compute the response and correlation functions as self-consistent averages over the effective two spin dynamics (14) (and drop the index 0).

At sufficiently high temperature, we expect the system to reach a time translational invariant state, in which two times observables only depend on the difference between the two times. This can be verified numerically by studying the auto-correlation function of the system $C(t_0 + \tau, t_0)$ for different values of the initial time t_0 , that after a short transient only depends on the time difference τ (Fig. 6).

Using the dynamical equations and the spherical constraint we can obtain an equation for the Lagrange multipliers:

$$\frac{1}{2} \frac{d}{dt} \frac{1}{N} \sum_i (s_i^a)^2 = 0 = \frac{1}{N} \sum_i s_i^a \dot{s}_i^a = \frac{1}{N} \sum_{i,j} s_i^a J_{ij} s_j^a - \ell_a \frac{1}{N} \sum_i (s_i^a)^2 + \frac{1}{N} \sum_i \sum_b \alpha \epsilon_{ab} s_i^a s_i^b + \frac{1}{N} \sum_i s_i^a \eta_i^a \quad (15)$$

$$\ell_a = \frac{1}{N} \sum_{i,j} s_i^a J_{ij} s_j^a + \sum_b \alpha \epsilon_{ab} C_{ab}(t = t') \quad (16)$$

There is a contribution that we can interpret as the average potential energy of each system, and one coming from the non-reciprocal interactions. Because of the symmetry of the system under the transformation $s_1 \rightarrow -s_2$, $s_2 \rightarrow s_1$, we expect the cross-correlation to be 0 at equal times, and the average potential energy to be the same in the two systems. Therefore the two Lagrange multipliers are equal in this regime, $\ell_1 = \ell_2 = \ell$. We expect this to be true as long as an extensive number of modes contribute to the dynamics, allowing us to interpret the sums as averages.

In the time-translational-invariant state, the DMFT equations greatly simplify in Fourier transform:

$$-i\omega s_a(\omega) = -\ell s_a(\omega) + \sum_b \alpha \epsilon_{ab} s_a(\omega) + \eta_a(\omega) + h_a(\omega) + \xi_a(\omega) + \sum_b R_{ab}(\omega) s_b(\omega) \quad (17)$$

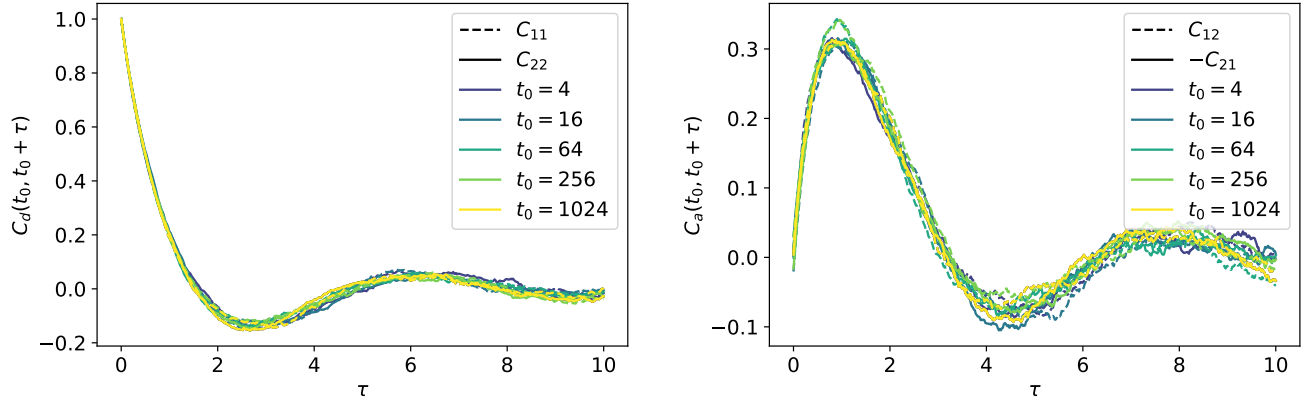


Figure 6: Auto-correlation function $C_d = C_{11} = C_{22}$ and cross-correlation function $C_a = C_{12} = -C_{21}$ for different values of the initial time t_0 , extracted from numerical simulations of the equations (1). $T = 1.4$, $\alpha = 1$, $N = 2000$, averaged over 5 runs of the simulations.

In matrix form we can express the result as:

$$((-i\omega + \ell)\mathbb{1} - R - \alpha\epsilon)\mathbf{s} = \xi + \eta + \mathbf{h} \quad (18)$$

Differentiating both sides with respect to \mathbf{h} we obtain:

$$((-i\omega + \ell)\mathbb{1} - R - \alpha\epsilon)R = \mathbb{1} \quad (19)$$

If we knew the Lagrange multiplier ℓ , this equation would determine R . Because of the aforementioned symmetry under the transformation $s_1 \rightarrow -s_2$, $s_2 \rightarrow s_1$, we have:

$$R_{11}(\omega) = R_{22}(\omega) = R_d(\omega) \quad R_{12}(\omega) = -R_{21}(\omega) = R_a(\omega) \quad (20)$$

$$R = \begin{pmatrix} R_d & R_a \\ -R_a & R_d \end{pmatrix} \quad (21)$$

We can then express the self-consistent equation on R in terms of R_d and R_a :

$$\begin{cases} R_d = \frac{\ell - i\omega - R_d}{(R_a + \alpha)^2 + (\ell - i\omega - R_d)^2} \\ R_a = \frac{R_a + \alpha}{(R_a + \alpha)^2 + (\ell - i\omega - R_d)^2} \end{cases} \quad (22)$$

This system of equations has 4 solutions, but only one has the correct $\alpha \rightarrow 0$ limit and decays for large ω .

All matrices of the form $\begin{pmatrix} M_d & M_a \\ -M_a & M_d \end{pmatrix}$ are diagonalized in the basis $v^\pm = \frac{1}{\sqrt{2}} \begin{pmatrix} \mp i \\ 1 \end{pmatrix}$. This leads to a simple expressions of the eigenvalues of R :

$$R_+ = R_d + iR_a \quad (23)$$

$$R_- = R_d - iR_a \quad (24)$$

We can write the self-consistent equation on R in its eigenbasis:

$$\ell - i(\omega + \alpha) - R_+ = R_+^{-1} \quad (25)$$

$$\ell - i(\omega - \alpha) - R_- = R_-^{-1} \quad (26)$$

$$R_+ = \frac{\ell - i(\omega + \alpha) - \sqrt{(\ell - i(\omega + \alpha))^2 - 4}}{2} \quad (27)$$

$$R_- = \frac{\ell - i(\omega - \alpha) - \sqrt{(\ell - i(\omega - \alpha))^2 - 4}}{2} \quad (28)$$

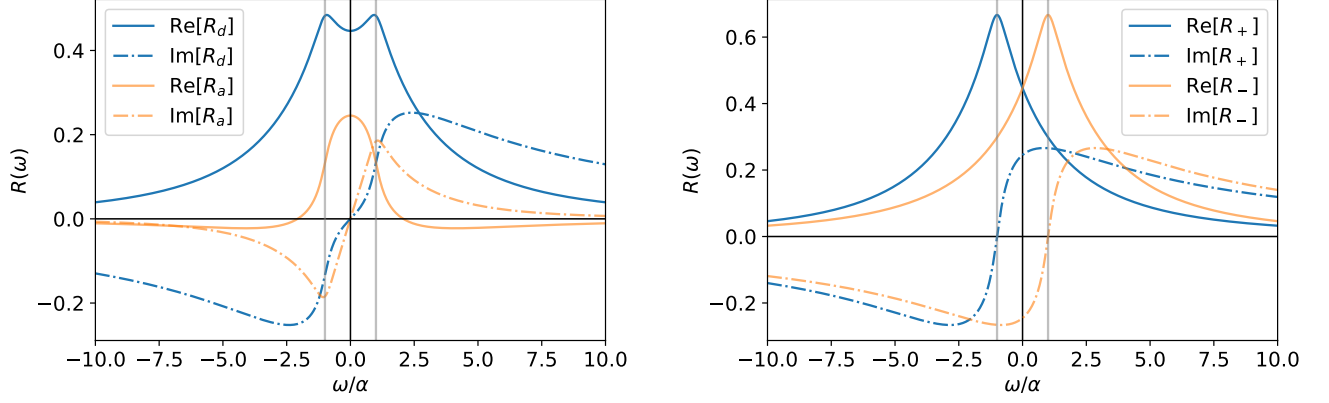


Figure 7: Real and imaginary parts of the matrix elements of the response function, in the original basis (left) and in the diagonalizing one (right). $T = 1.5$, $\alpha = 0.7$, $\omega = \alpha$ indicated in gray.

As noted in the main text, these equations are the same that would be found in the uncoupled case, except for a shift of $\pm\alpha$ in ω .

Because the problem is linear, $\mathbf{s}(\omega) = R(\omega)(\xi(\omega) + \eta(\omega))$. This allows us to compute the correlation functions:

$$\delta(\omega + \omega')C(\omega) = \langle \mathbf{s}(\omega)\mathbf{s}(\omega')^T \rangle = \langle R(\omega)(\xi(\omega) + \eta(\omega))(R(\omega')(\xi(\omega') + \eta(\omega'))^T) \rangle = \quad (29)$$

$$= R(\omega)\langle (\Xi(\omega) + \eta(\omega))(\Xi(\omega') + \eta(\omega'))^T \rangle R(\omega')^T = \quad (30)$$

$$= \delta(\omega + \omega')R(\omega)(C(\omega) + 2T)R^\dagger(\omega) \quad (31)$$

This gives us the self-consistent equation on C :

$$R^{-1}C(R^\dagger)^{-1} - C = 2T \quad (32)$$

As R , also C is of the form:

$$C(\omega) = \begin{pmatrix} C_d(\omega) & C_a(\omega) \\ -C_a(\omega) & C_d(\omega) \end{pmatrix} \quad (33)$$

This means that it is diagonalized in the same basis v^\pm as R , which ensures that C and R commute. We then obtain:

$$C(\omega)((R(\omega)^\dagger R(\omega))^{-1} - \mathbb{1}) = 2T \quad (34)$$

If $(R(\omega)^\dagger R(\omega))^{-1} - \mathbb{1}$ is invertible,

$$C(\omega) = 2T((R(\omega)^\dagger R(\omega))^{-1} - \mathbb{1})^{-1} \quad (35)$$

Using again the diagonalizing basis, we have:

$$C_\pm(\omega) = \frac{2T}{|R_\pm(\omega)|^{-2} - 1} \quad (36)$$

This is again the same equation as in the uncoupled case. Because the ω dependence is only through R_\pm , also C behaves in the same way as in the uncoupled case except for the $\pm\alpha$ shift in ω .

The spherical constraint imposes that $C_d(t=0) = 1$:

$$C_d(t=0) = \frac{1}{2\pi} \int d\omega C_d(\omega) = \frac{1}{2\pi} \int d\omega C_\pm(\omega) = \frac{1}{2\pi} \int d\omega C_{\alpha=0}(\omega) = 1 \quad (37)$$

We have used the fact that C_a is an odd function of ω , and therefore does not contribute to the integral. Because the non-reciprocal coupling only introduces a shift in ω , it does not change the integral either. The equation imposed by the spherical constraint determines the Lagrange multiplier ℓ , which will therefore be at all temperatures the same as

in the uncoupled case. This leads to the same critical point $T_c = 1$, where $\ell \rightarrow 2$ and touches the edge of the spectrum of J .

Note the crucial role of the singularities of R and C for $\ell = 2$ for obtaining a critical point at finite temperature. For $\ell = 2$ one eigenvalue of R behaves around $\omega = \alpha$ as $1 - \sqrt{|\omega - \alpha|}$. The corresponding eigenvalue of C therefore behaves as $2T|\omega - \alpha|^{-1/2}$, leading to an integrable singularity. If this was not the case (as for example in reference [40]), the integral in equation (37) would be diverging at criticality, implying that criticality can only be reached at 0 temperature.

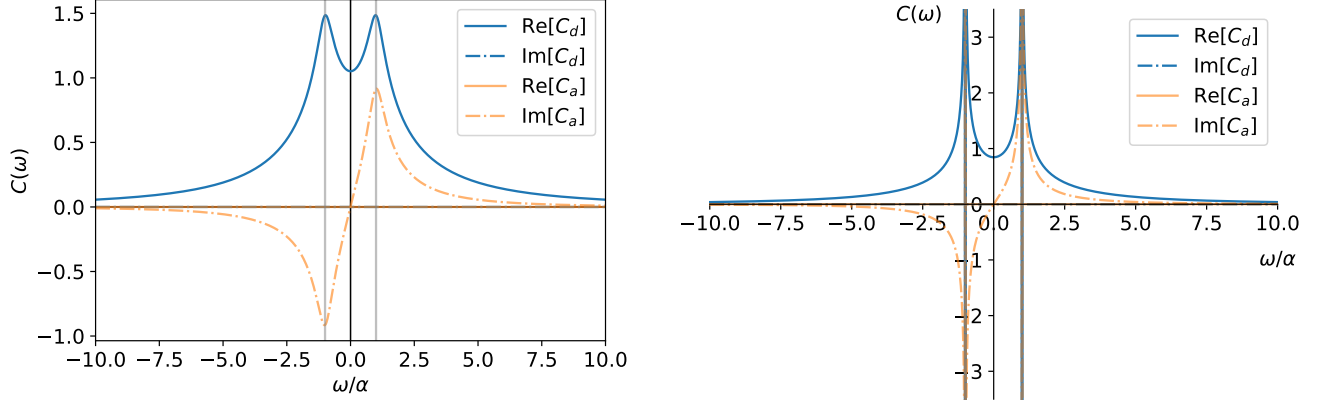


Figure 8: Real and imaginary parts of the correlation functions, for $T = 1.5$ (left) and for $T = T_c = 1$ (right). $\alpha = 0.7$, $\omega = \alpha$ indicated in gray.

Aging

In order to study the aging behavior of our system, it is convenient to look at it in the basis that diagonalizes the interaction matrix J :

$$\dot{\mathbf{s}}_\mu = (\mu\mathbb{1} - \Lambda + \alpha\epsilon)\mathbf{s}_\mu + \xi_\mu \quad (38)$$

In this basis different modes are only coupled through the Lagrange multipliers. We can formally write the solution in terms of the realization of the noise $\xi_\mu(t)$ and the (unknown) time evolution of the Lagrange multipliers:

$$\mathbf{s}_\mu(t) = e^{(\mu\mathbb{1} + \alpha\epsilon)t - \int_0^t \Lambda(t')dt'} \mathbf{s}_\mu(0) + \int_0^t dt' e^{(\mu\mathbb{1} + \alpha\epsilon)(t-t') - \int_{t'}^t \Lambda(t'')dt''} \xi_\mu(t') \quad (39)$$

On time scales that do not diverge with N , an extensive number of modes will contribute to the dynamics of the Lagrange multipliers. As before, and because of the randomness in the initial conditions, we then expect them to be equal at all times, $\ell_1(t) = \ell_2(t) = \ell(t)$. This greatly simplifies the analysis, because now Λ and ϵ commute and we can separate their exponentials:

$$\mathbf{s}_\mu(t) = e^{\mu t - \int_0^t \ell(t')dt'} R_{\alpha t} \mathbf{s}_\mu(0) + \int_0^t dt' e^{\mu(t-t') - \int_{t'}^t \ell(t'')dt''} R_{\alpha(t-t')} \xi_\mu(t') \quad (40)$$

We have introduced the rotation matrix $R_{\alpha t} = e^{\alpha\epsilon t} = \begin{pmatrix} \cos \alpha t & \sin \alpha t \\ -\sin \alpha t & \cos \alpha t \end{pmatrix}$.

We can express the initial conditions in polar coordinates: $\mathbf{s}^\mu(0) = r_\mu(0) \begin{pmatrix} \sin \theta_\mu(0) \\ \cos \theta_\mu(0) \end{pmatrix}$. We consider uniform initial conditions on the two spheres, which corresponds to taking uniform and independent $\theta_\mu(0)$.

In order to find an equation for $\ell(t)$, we use the spherical constrain on system 1:

$$N = \left\langle \sum_{\mu} (s_{\mu}^1(t))^2 \right\rangle = \sum_{\mu} e^{2\mu t - 2 \int_0^t \ell(t') dt'} \sin^2(\theta_{\mu}(0) + \alpha t) r_{\mu}^2(0) + \quad (41)$$

$$+ \sum_{\mu} \int_0^t dt' dt'' e^{\mu(t-t') - \int_{t'}^t \ell(\tau) d\tau} e^{\mu(t-t'') - \int_{t''}^t \ell(\tau') d\tau'}. \quad (42)$$

$$\cdot \langle (\cos \alpha(t-t') \xi_{\mu,1}(t') + \sin \alpha(t-t') \xi_{\mu,2}(t')) (\cos \alpha(t-t'') \xi_{\mu,1}(t'') + \sin \alpha(t-t'') \xi_{\mu,2}(t'')) \rangle = \quad (43)$$

$$= \frac{1}{2} \sum_{\mu} e^{2\mu t - 2 \int_0^t \ell(t') dt'} r_{\mu}^2(0) + \quad (44)$$

$$+ 2T \sum_{\mu} \int_0^t dt' e^{2\mu(t-t') - 2 \int_{t'}^t \ell(\tau) d\tau} (\cos^2 \alpha(t-t') + \sin^2 \alpha(t-t')) = \quad (45)$$

$$= \frac{N}{2} \int d\mu \rho(\mu) e^{2\mu t - 2 \int_0^t \ell(t') dt'} r_{\mu}^2(0) + 2TN \int d\mu \rho(\mu) \int_0^t dt' e^{2\mu(t-t') - 2 \int_{t'}^t \ell(\tau) d\tau} \quad (46)$$

As expected, we would have obtained the same result using system 2, self-consistently confirming that $\ell_1(t) = \ell_2(t) = \ell(t)$. We have neglected all terms that do not contribute when averaging over the initial conditions or the noise, and used $\langle r_{\mu}^2(0) \rangle = \langle s_{\mu}^2(0) \rangle + \langle \sigma_{\mu}^2(0) \rangle = 2$. $\rho(\mu)$ is the eigenvalue density of J , given by the Wigner semicircle:

$$\rho(\mu) = \frac{1}{2\pi} \sqrt{4 - \mu^2}, \quad \mu \in [-2, 2] \quad (47)$$

Imposing that the constrain is satisfied at all times we obtain:

$$\int d\mu \rho(\mu) e^{2\mu t - 2 \int_0^t \ell(t') dt'} + 2T \int d\mu \rho(\mu) \int_0^t dt' e^{2\mu(t-t') - 2 \int_{t'}^t \ell(\tau) d\tau} = 1 \quad (48)$$

This is the same equation on the Lagrange multiplier that would be obtained in the uncoupled case [43], therefore we can use the known result for the spherical constraint.

We can now compute the correlation function:

$$C(t, t') = \left\langle \sum_{\mu} \mathbf{s}_{\mu}(t) \mathbf{s}_{\mu}(t')^T \right\rangle = \sum_{\mu} e^{\mu t - \int_0^t \ell(\tau) d\tau} e^{\mu t' - \int_0^{t'} \ell(\tau') d\tau'} R_{\alpha t} \mathbf{s}_{\mu}(0) (R_{\alpha t'} \mathbf{s}_{\mu}(0))^T + \quad (49)$$

$$+ \sum_{\mu} \int_0^t dz \int_0^{t'} dz' e^{\mu(t-z) - \int_z^t \ell(\tau) d\tau} e^{\mu(t'-z') - \int_{z'}^{t'} \ell(\tau') d\tau'} \langle R_{\alpha(t-z)} \xi_{\mu}(z) (R_{\alpha(t'-z')} \xi_{\mu}(z'))^T \rangle = \quad (50)$$

$$= \int d\mu \rho(\mu) e^{\mu(t+t') - \int_0^t \ell(\tau) d\tau - \int_0^{t'} \ell(\tau') d\tau'} R_{\alpha(t-t')} + \quad (51)$$

$$+ \int d\mu \rho(\mu) \int_0^t dz \int_0^{t'} dz' e^{\mu(t-z) - \int_z^t \ell(\tau) d\tau} e^{\mu(t'-z') - \int_{z'}^{t'} \ell(\tau') d\tau'} R_{\alpha(t-t')} = \quad (52)$$

$$= \left(\int d\mu \rho(\mu) e^{\mu(t+t') - \int_0^t \ell(\tau) d\tau - \int_0^{t'} \ell(\tau') d\tau'} + \int d\mu \rho(\mu) \int_0^t dz \int_0^{t'} dz' e^{\mu(t-z) - \int_z^t \ell(\tau) d\tau} e^{\mu(t'-z') - \int_{z'}^{t'} \ell(\tau') d\tau'} \right). \quad (53)$$

$$\cdot R_{\alpha(t-t')} \quad (54)$$

The factor in parentheses is precisely the expression that can be derived for the correlation function in the uncoupled case $C_0(t, t')$ [43]. Therefore we find:

$$C(t, t') = C_0(t, t') R_{\alpha(t-t')} \quad (55)$$

This form is in very good agreement with the result of numerical simulations, shown in Figure 9.

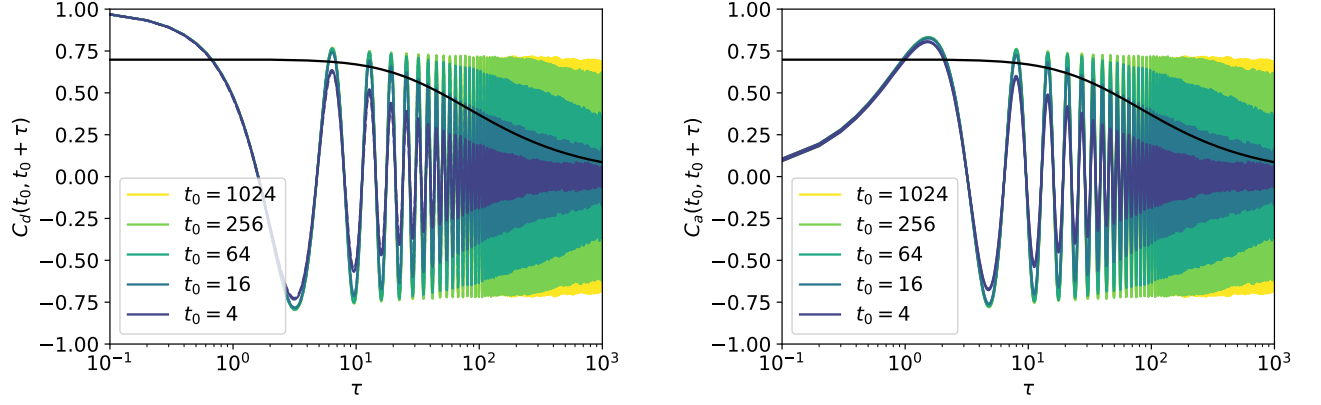


Figure 9: Diagonal (left) and off-diagonal (right) component of the correlation function for different values of t' measured in numerical simulations of equation 1. In black the envelope of the oscillations (i.e. $C_0(t, t')$) for $t' = 16$. $T = 0.3$, $N = 20000$. $q_{EA} = 0.7$.

Stability of equilibrium points

In order to better understand the behavior of our system at long times, we can look at the fixed points of the deterministic dynamics ($T = 0$). It is convenient to use again the basis that diagonalizes the interaction matrix J :

$$\begin{cases} \dot{s}_\mu^1 = (\mu - l_1) s_\mu^1 + \alpha s_\mu^2 = 0 \\ \dot{s}_\mu^2 = (\mu - l_2) s_\mu^2 - \alpha s_\mu^1 = 0 \end{cases} \quad (56)$$

We have $4N$ stationary points; in each only one of the modes μ^* contributes:

$$s_\mu^1 = \pm s_\mu^2 = \pm \sqrt{N} \delta_{\mu, \mu^*} \quad (57)$$

Let us consider a fixed point \mathbf{s}^* with positive projections on the mode μ^* for both clones (the other equilibria are completely equivalent thanks to the symmetries of the system). Imposing stationarity in Eq. (56) and choosing the signs in Eq. (57) determines the Lagrange multipliers

$$\ell_1 = \mu^* + \alpha \quad \ell_2 = \mu^* - \alpha \quad (58)$$

Note that $\ell_1 \neq \ell_2$ in this particular case.

To study the stability of this fixed point we can look at the linearized dynamics:

$$\delta \mathbf{s}_\mu = \mathbf{s}_\mu - \mathbf{s}_\mu^* \quad (59)$$

$$\delta \dot{\mathbf{s}}_\mu = M_\mu \delta \mathbf{s}_\mu \quad (60)$$

$$M_\mu = \begin{pmatrix} \mu - \mu^* - \alpha & \alpha \\ -\alpha & \mu - \mu^* + \alpha \end{pmatrix} \quad (61)$$

The stability matrix M_μ has only one eigenvalue $\lambda_\mu = \mu - \mu^* = \Delta\mu$, with only one associated independent eigenvector: it is a *defective* matrix. If μ^* is not the maximum eigenvalue, a finite number of the stability eigenvalues λ_μ will be positive, and therefore the system will depart exponentially from the fixed point. If μ^* is the maximum eigenvalue, all the stability eigenvalues will be negative, except for the one associated with mode μ^* which will be zero. Nevertheless, because M_μ is defective, even in this case we are not guaranteed that a small perturbation around the fixed point will be exponentially damped. Indeed, we can explicitly solve the linearized equation:

$$\delta \mathbf{s}^\mu = e^{M_\mu t} \delta \mathbf{s}^\mu(0) = \begin{pmatrix} e^{\Delta\mu t} (1 - \alpha t) & \alpha e^{\Delta\mu t} t \\ -\alpha e^{\Delta\mu t} t & e^{\Delta\mu t} (1 + \alpha t) \end{pmatrix} \delta \mathbf{s}^\mu(0) \quad (62)$$

Even though at long times the behavior is controlled by the decaying exponential, at short times we can indeed see a growth of the perturbation. To clarify this point we can expand the exponential:

$$\delta \mathbf{s}^\mu \sim \begin{pmatrix} 1 + (\Delta\mu - \alpha)t & \alpha t \\ -\alpha t & 1 + (\Delta\mu + \alpha)t \end{pmatrix} \delta \mathbf{s}^\mu(0) \quad (63)$$

Let us take for example the perturbation $\delta \mathbf{s}^\mu(0) = \varepsilon \begin{pmatrix} 0 \\ 1 \end{pmatrix}$. Because the two clones are perfectly aligned, while clone 2 would like to be antialigned with clone 1, we expect that this perturbation on clone 2 could destabilize the system. Indeed at short times we obtain $\delta \mathbf{s}^\mu(t) = \varepsilon \begin{pmatrix} \alpha t \\ 1 + (\Delta\mu + \alpha)t \end{pmatrix}$.

Random α

In order to investigate whether the introduction of a continuous distribution of oscillations timescales can destroy aging we modify our system to consider random independent values of the non-reciprocal coupling α_i for each pair of spins s_i^1, s_i^2 . The dynamical equation becomes:

$$\dot{s}_i^a = \sum_{j=1}^N J_{ij} s_j^a - \ell_a s_i^a + \sum_b \alpha_i \epsilon_{ab} s_i^b + \eta_i^a + h_i^a \quad (64)$$

We can replicate the DMFT computation as in the previous case. The main difference is that the response and correlation functions are now α -dependent, but only their average enters the effective two-spin equations. We will indicate with R_α and C_α the α -dependent quantities, and with R and C their average over α . The DMFT equations read:

$$\dot{s}^a = -\ell_a s^a + \sum_b \alpha \epsilon_{ab} s^b + \eta^a + h^a + \xi^a + \sum_b \int^t dt' R_{ab}(t, t') s^b(t') \quad (65)$$

$$\langle \xi^a(t) \xi^b(t') \rangle = C_{ab}(t, t') \quad (66)$$

An analogous computation to the previous one now gives:

$$R(\omega) = \overline{((-i\omega + \ell)\mathbb{1} - R - \alpha\epsilon)^{-1}} \quad (67)$$

$$C(\omega) = 2T \left(\overline{(R^\alpha(\omega)^\dagger R^\alpha(\omega))^{-1}} - \mathbb{1} \right)^{-1} \quad (68)$$

We have indicated with an overline the average over α .

As before, C would have a critical point if $\overline{(R^\alpha(\omega)^\dagger R^\alpha(\omega))}$ had an eigenvalue equal to 1. Nevertheless, while before when this happened R also had a singularity in $\omega = \pm\alpha$, this singularity is now smoothed out by the integration over α . This means that at the critical point C would behave as $1/\omega$. Because this singularity would not be integrable, in order to satisfy the spherical constraint $C_d(t=0) = 1$ this cannot happen at finite temperature.

In the case of a Gaussian and centered distribution of the α it is possible to compute analytically the response and correlation functions at all temperatures.

Different interaction matrices

In many cases, it could be more realistic to consider two different interaction matrices for the two species. We consider the case in which there is any amount of correlation between J_{ij}^1 and J_{ij}^2 :

$$\overline{J_{ij}^a J_{ij}^b} = \frac{1}{N} (\delta_{ab} + (1 - \delta_{ab})\rho) \quad (69)$$

The dynamical equation becomes:

$$\dot{s}_i^a = \sum_j J_{ij}^a s_j^a - \ell_a s_i^a + \alpha \sum_b \epsilon_{ab} s_i^b + \eta_i^a + h_i^a \quad (70)$$

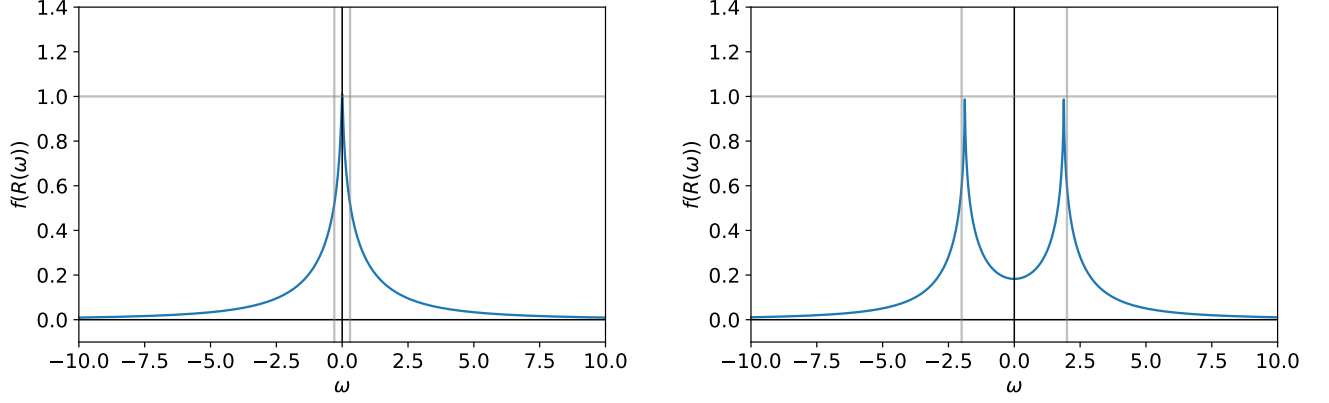


Figure 10: $f(R)$ defined in eq. (78) at the critical point (i.e. when it reaches 1) for $\rho = 0$, $\alpha = 0.3 < \alpha^*(0)$ (left) and $\alpha = 2$ (right). In both cases the functions are analytic, but very close to being singular at their peaks.

We can replicate the DMFT computation as in the previous cases. The main difference is that some ρ factors pop up in the off-diagonal components of the memory terms and of the correlation of the noise:

$$\dot{s}^a = -l_a s^a + \sum_b \epsilon_{ab} \alpha s^b + \eta^a + h^a + \xi_a + \int_0^t dt' R_{aa}(t, t') s^a(t') + \sum_b (1 - \delta_{ab}) \rho \int_0^t dt' R^{ab}(t, t') s^b(t') \quad (71)$$

$$\langle \xi_a(t) \xi_b(t') \rangle = N \overline{J_{0j}^a J_{0j}^b} \mathbb{E} [s_i^a(t) s_i^b(t')] = \delta_{ab} C_{aa}(t, t') + (1 - \delta_{ab}) \rho C_{ab}(t, t') \quad (72)$$

In order to write down in matrix form the self-consistent equations on R and C , it is convenient to define the matrices:

$$\tilde{R} = \begin{pmatrix} R_d & \rho R_a \\ -\rho R_a & R_d \end{pmatrix} \quad \tilde{C} = \begin{pmatrix} C_d & \rho C_a \\ -\rho C_a & C_d \end{pmatrix} \quad (73)$$

The self-consistent equations, obtained as before, then read:

$$R = ((-i\omega + l)\mathbb{1} - \tilde{R} - A)^{-1} \quad (74)$$

$$C(\omega) = (2T + \tilde{C}(\omega))R(\omega)R^\dagger(\omega) \quad (75)$$

At small but finite α the response and correlation functions are peaked in $\omega = 0$ at all temperatures, whereas for $\alpha > \alpha^*(\rho)$ they develop two symmetric peaks at finite values of ω (Figure 10), signaling a damped oscillating behavior as in the case in which the two species have the same J . For $\rho = 0$ the equations simplify, and we can show that this crossover occurs at $\alpha^*(0) = 1/\sqrt{8}$.

The system has a critical point when the correlation function diverges. The solution for the diagonal and off-diagonal elements of C read:

$$C_d(\omega) = 2T \frac{|R_d|^2 + |R_a|^2 - \rho|R_d^2 + R_a^2|^2}{1 - ((\rho + 1)(|R_d|^2 + |R_a|^2) - \rho|R_d^2 + R_a^2|^2)} \quad (76)$$

$$C_a(\omega) = 2T \frac{R_a R_d^* - R_d R_a^*}{1 - ((\rho + 1)(|R_d|^2 + |R_a|^2) - \rho|R_d^2 + R_a^2|^2)} \quad (77)$$

Therefore the critical point will be when

$$f(R) = (\rho + 1)(|R_d|^2 + |R_a|^2) - \rho|R_d^2 + R_a^2|^2 = 1 \quad (78)$$

At any value of $\rho < 1$, when this condition is met the response function is not singular. As discussed before, this means that the system does not have a critical point at any finite temperature. Nevertheless, both for small ($\alpha \lesssim 0.3$) and large ($\alpha \gtrsim 1$) values of α , the response function is extremely close to being critical (Figure 10): in fact it would become critical for (unphysical) values of the Lagrange multipliers just below those reached when the correlation function diverges. This means that at moderate system sizes and not too long times the situation would be indistinguishable from a real phase transition to a spin glass phase at small α and an amorphous oscillating one at large α .

Coupling magnetization

Another possible coupling mechanism between the two clones is through their magnetization. Without ferromagnetic interactions inside each clone the magnetization is zero throughout the phase diagram, therefore the addition of non-reciprocity has no effect at all. Let us then consider the case in which each spin wants to align with the magnetization of its own clone, and either align or antialign with the magnetization of the other:

$$\dot{s}_i^a = \sum_j J_{ij} s_j^a - \ell_a s_i^a + \frac{\alpha_+}{N} \sum_j s_j^a + \sum_b \epsilon_{ab} \frac{\alpha_-}{N} \sum_j s_j^b \quad (79)$$

α_+ and α_- are the strengths of the reciprocal and non-reciprocal interactions, we do not consider thermal fluctuations. The system exhibits a quite rich phenomenology. Its phase diagram is represented in Figure 11, with different observables represented by the colormaps. The same observables are also plotted as a function of α_- at constant $\alpha_+ = 1.7$ in Figure 12.

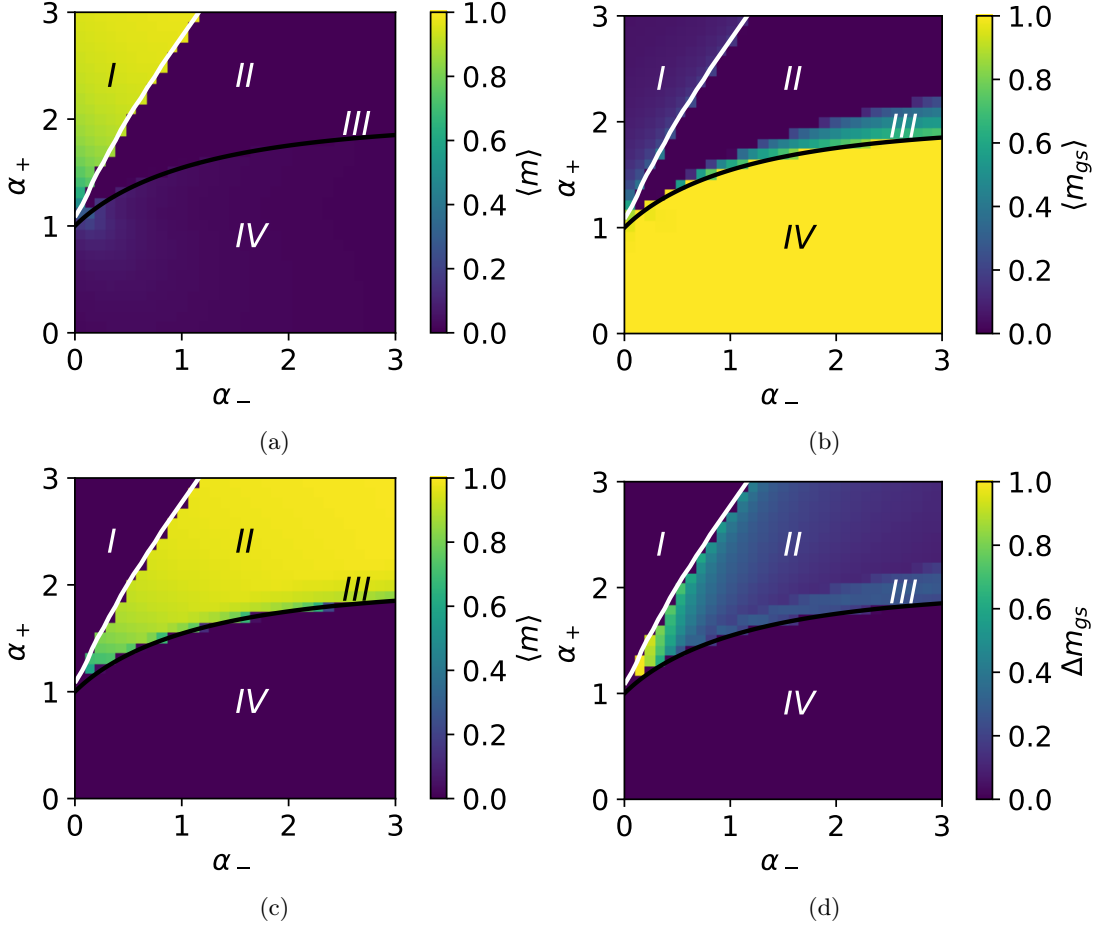


Figure 11: 4 phases: one with $\langle m \rangle = 0$, $\langle m_{gs} \rangle \sim 1$ (m_{gs} is the projection of s on the leading eigenvector of J), one in which the magnetizations oscillate periodically ($\Delta m > 0$, $\Delta m = \max(m) - \min(m)$ in last 100 time units) and $\langle m_{gs} \rangle = 0$, one in which m_{gs} oscillates around a non zero value, one with finite static magnetization ($m > 0$, $\Delta m = 0$). α_- stabilizes the non magnetized state close to $\alpha_+ = 1$, α_+ stabilizes the magnetized fixed point, so that at higher α_+ we need higher α_- to start oscillations. The black line indicates condition (85), the white line the disappearance of the solution of eq. (86). $N = 1500$, same J for all points.

At small values of α_+ (phase IV in the figures), the non-reciprocity plays no role, and the system converges at long times to the leading eigenvector of the interaction matrix. The absolute value of the projection of each of the clones on this eigenvector, m_{gs} , is asymptotically equal to 1 (Figure 11b). The dynamics is very similar to the one that we would find without non-reciprocity: the system exhibits aging. We can study the stability of this fixed point solution

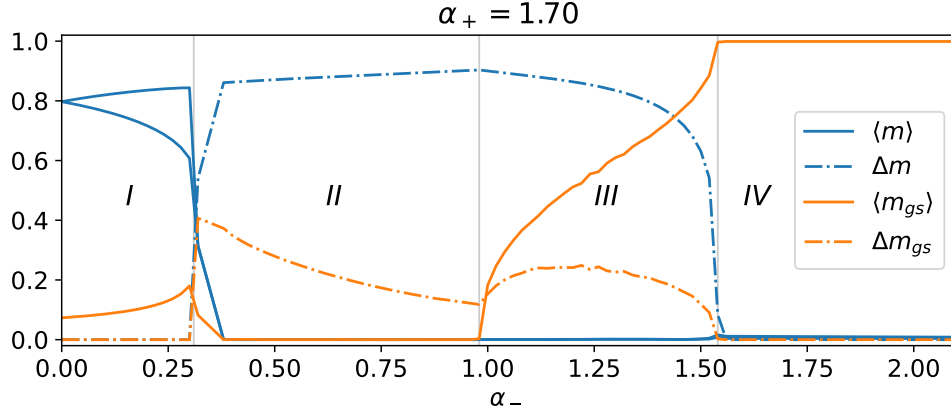


Figure 12: Order parameters as a function of α_- at fixed $\alpha_+ = 1.7$. $N = 4000$.

by linearizing around it:

$$\delta \dot{s}_i^a = \sum_j J_{ij} \delta s_j^a - \ell \delta s_i^a + \frac{\alpha_+}{N} \sum_j \delta s_j^a + \sum_b \epsilon_{ab} \frac{\alpha_-}{N} \sum_j \delta s_j^b \quad (80)$$

At the fixed point $l_1 = l_2 = l = 2$. We define the $(2N \times 2N)$ stability matrix M such that

$$\delta \dot{\mathbf{s}} = M \delta \mathbf{s} \quad (81)$$

The fixed point is unstable if M has a positive eigenvalue. The eigenvalues of M are the poles of its resolvent:

$$G(z) = (z\mathbb{1} - M)^{-1} \quad (82)$$

If an instability occurs, because it would be due to the magnetization-mediated interactions, we expect the unstable mode to have some overlap with the vector of the fully magnetized states, $|1_1\rangle$ and $|1_2\rangle$. We project the resolvent on this 2-dimensional space

$$\langle 1_s, 1_\sigma | G(z) | 1_s, 1_\sigma \rangle = \frac{1}{(z + \ell - g(z + \ell))\mathbb{1} - \begin{pmatrix} \alpha_+ & \alpha_- \\ -\alpha_- & \alpha_+ \end{pmatrix}} \quad (83)$$

$g(z) = \frac{z - z\sqrt{1-4/z^2}}{2}$ is the Stieltjes transform of J [85]. Solving for the poles of the projected resolvent we find:

$$z = -\ell + \alpha_+ \left(1 + \frac{1}{\alpha_+^2 + \alpha_-^2} \right) \pm i\alpha_- \left(1 - \frac{1}{\alpha_+^2 + \alpha_-^2} \right) \quad (84)$$

The real part of the eigenvalue becomes positive when

$$\alpha_+ \left(1 + \frac{1}{\alpha_+^2 + \alpha_-^2} \right) = 2 \quad (85)$$

This condition is plotted in black in Figure 11, it perfectly agrees with numerical results. For non-zero α_- the transition is retarded, and when it occurs the unstable eigenvalue is complex. For $\alpha_- = 0$ we recover the known result for the phase transition to a ferromagnetic state at $\alpha_+ = 1$; for $\alpha_- \rightarrow \infty$ the ground state of the interaction matrix loses stability at $\alpha_+ = 2$.

At very strong values of α_+ (phase I in the figures) the system converges to a fixed point with finite magnetizations m_1 and m_2 . At the fixed point the magnetizations and the Lagrange multipliers satisfy:

$$\begin{cases} (\alpha_+^2 + \alpha_-^2)g(\ell_1)g(\ell_2) - \alpha_+(g(\ell_1) + g(\ell_2)) + 1 = 0 \\ m_1 = \frac{\alpha_- g(\ell_1)}{1 - \alpha_+ g(\ell_2)} m_2 \\ (\alpha_+ m_1 + \alpha_- m_2)^2 \frac{g(\ell_1)}{\sqrt{\ell_1^2 - 4}} = 1 \\ (\alpha_+ m_2 - \alpha_- m_1)^2 \frac{g(\ell_2)}{\sqrt{\ell_2^2 - 4}} = 1 \end{cases} \quad (86)$$

Studying when this system of equations stops having a solution, we find the phase boundary of the magnetized phase, indicated in white in Figure 11. Again there is very good agreement with numerical simulations.

Between the two phases described so far, there is an extended region in which the system exhibits strong oscillations. This region is actually composed of two phases: one in which each clone rotates around the origin (phase *II* in the figures), and one in which each clone rotates around a vector with a finite projection on the leading eigenvector of J (phase *III* in the figures). By Principal Component Analysis we see that in phase *II* the system explores a space spanned by 2 vectors, whereas in phase *III* it explores a space spanned by 3 vectors. Also in phase *III* we encounter aging behaviour.

Non-reciprocal p-spin model

As a first step in the study of non-reciprocal aging in more complex glassy systems, we studied numerically the dynamics of two non-reciprocally coupled p-spin systems, for $p = 3$ [82, 83]:

$$\dot{s}_i^a = \frac{1}{2} \sum_{i_2, i_3}^N J_{i, i_2, i_3} s_{i_2}^a s_{i_3}^a - \ell_a s_i^a + \sum_b \alpha \epsilon_{ab} s_i^b + \eta_i^a \quad (87)$$

The simulations are numerically challenging because the 3-body fully connected interactions lead to a scaling as N^3 of the simulation time. For this reason, we could only explore moderate system sizes ($N = 100$) and times ($t_{max} = 600$).

In Figure 13 we plot the autocorrelation function for different waiting times t_0 as a function of the time interval τ . For $\alpha = 0$ (top) the system exhibits aging both at $T = 0.1$ (left) and at $T = 0.5$ (right). Indeed the dynamical phase transition temperature for this model is $T_d = \sqrt{\frac{p(p-2)^{p-2}}{2(p-1)^{p-1}}} \approx 0.61$. For strong non-reciprocal coupling ($\alpha = 1$, bottom), aging is suppressed at both temperatures: the correlation functions reach a time-translational invariant regime, in which they decay on the timescale associated with the non-reciprocity $\frac{2\pi}{\alpha}$. Nevertheless, at moderate values of the non-reciprocal coupling ($\alpha = 0.3$, middle), we see that the correlation functions do not reach a time-translational invariant regime (at least at $T = 0.1$) and in particular do not decay on the timescale $\frac{2\pi}{\alpha}$. This is an indication that aging could survive the introduction of a finite but moderate non-reciprocity, possibly under an interaction-dependent dynamical temperature $T_d(\alpha)$.

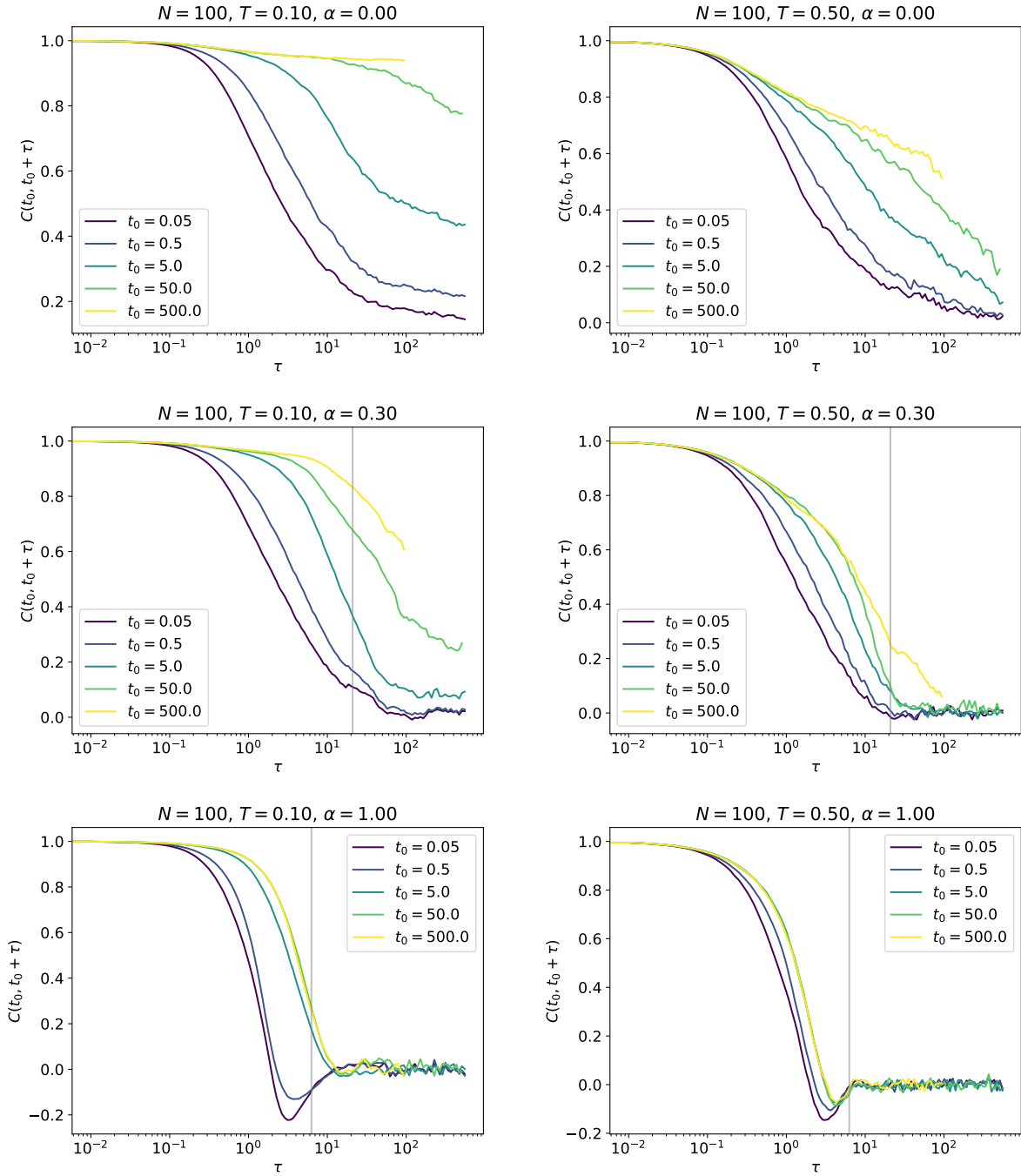


Figure 13: Correlation function in log time, averaged over 55 runs with the same interaction tensor J . The grey line represents the timescale associated with the non reciprocity $\frac{2\pi}{\alpha}$.